

Targeting DNA-PK is a highly conserved poxvirus innate immune evasion mechanism

Marisa Oliveira^{1†}, Paul T. Manna^{2†}, Damaris Ribeiro-Rodrigues³, Thomas Allport⁴, Emma Wagner¹, Heather Brooks³, Michael A. Skinner⁵, Efstathios S. Giotis^{5,6}, Amanda K. Chaplin⁴, Rodrigo Guabiraba^{7*}, Clare E. Bryant^{3*}, Brian J. Ferguson^{1*}

¹Department of Pathology, University of Cambridge, Cambridge, United Kingdom

²Department of Physiology, University of Gothenburg, Gothenburg, Sweden

³Department of Veterinary Medicine, University of Cambridge, Cambridge, United Kingdom

⁴Leicester Institute for Structural and Chemical Biology, Department of Molecular and Cell Biology, University of Leicester, Leicester, United Kingdom

⁵Department of Infectious Diseases, Imperial College London, London, United Kingdom

⁶School of Life Sciences, University of Essex, Colchester, United Kingdom

⁷ISP, INRAE, Université de Tours, Nouzilly, France

*Corresponding authors: Clare Bryant ceb27@cam.ac.uk, Rodrigo Guiabiraba rodrigo.guabiraba-brito@inrae.fr, Brian Ferguson bf234@cam.ac.uk

† These authors contributed equally to this work

Abstract

The sensing of viral nucleic acid by pattern recognition receptors (PRRs) is essential for initiation of a type-I interferon response against infection. Intracellular DNA sensing PRRs are responsible for initiating innate immune responses to poxviruses and other double-stranded DNA viruses. Poxviruses, in turn, encode an armoury of immunomodulators that inhibit this host defence mechanism. DNA-dependent protein kinase (DNA-PK) is an essential component of the cGAS/STING-dependent viral DNA sensing machinery that leads to the initiation of a type-I interferon response during poxvirus infection. Poxviruses counter this host sensing mechanism using the C4/C10 family of proteins that target DNA-PK, interfering with its ability to bind viral DNA. Although the DNA-PK complex, known also for its role in double strand break repair, is conserved across multiple taxa, its function in innate immunity outside mammals is unexplored. Here we analysed the contribution of DNA-PK to poxvirus DNA sensing in chickens, a species that is evolutionarily distant from mammals, but that is also infected by poxviruses. We found that DNA-PK functions as a DNA sensor in chickens, and this process is countered by C4/C10 family members found in fowlpox virus. This host/pathogen interaction is conserved across a broader range of species than other mechanisms of poxvirus antagonism of innate immune sensing, which may reflect the difficulty of the host in evolving escape mechanisms that interfere with a protein that is essential for maintenance of genomic stability.

Introduction

The molecular arms race between host and pathogen results in the evolution of increasing complexity in both host immune systems and pathogen effector mechanisms [1,2]. This competition is exemplified by the interplay between host innate immune responses and antagonists of these systems deployed by viruses that provide extensive selective pressure, shaping the evolution of host immune responses [3,4]. Across all vertebrate taxa, pattern recognition receptors (PRRs) have evolved to sense infection by directly binding molecular components of pathogens. PRR signalling activation results in the rapid transcription of antimicrobial genes, including interferons and cytokines in mammals. Viral effector mechanisms target PRR signalling to effectively block the production of these inflammatory mediators, allowing them to increase the temporal window for their replication and spread. Determination of the mechanisms of antiviral innate immunity in species that cross different orders of life has significant implications both for understanding the evolution of host/pathogen interactions and for understanding the outcome of zoonotic viral disease severity.

Intracellular PRRs that sense and respond to nucleic acids are of particular importance in initiating the host response to virus infection [5]. The DNA sensing PRRs initiate interferon transcription following DNA virus infections by sensing viral genomic DNA. A number of viral DNA sensors have been identified that are critical for defence against DNA viruses. These sensors, including cGAS and DNA-PK drive the STING-dependent IRF and NF- κ B activation responsible for initiating an antiviral transcriptional programme [6]. Multiple families of DNA viruses are detected by PRRs that activate STING, including *poxviridae*, *herpesviridae* and *adenoviridae*, and these virus families encode multiple inhibitors of DNA sensing pathways that significantly reduce the production of interferons and cytokines from infected cells [7–9].

Poxviruses are an ancient virus family whose members can infect invertebrates, birds, reptiles and mammals. Poxviruses have rapid, lytic life cycles, necessitating extensive interactions with host innate immune systems. In mammals, poxviruses trigger cGAS and DNA-PK-dependent interferon production via STING [9–11] but encode an armoury of proteins that target this intracellular signalling pathway so effectively that the wild type virus elicits little to no interferon production from infected cells [9,12–14]. The effective inhibition of viral DNA sensing PRRs is achieved by several families of proteins that each inhibit a different step in these signalling pathways. Vaccinia virus (VACV) is perhaps the best studied poxvirus in terms of immune evasion mechanisms [14–16]. VACV

encodes several defined inhibitors of DNA PRRs including the C4/C10 family that binds the Ku70/80 component of DNA-PK and sterically impedes DNA-binding to reduce viral DNA-driven interferon production from infected cells [17–19]. The C10 protein, in the VACV Copenhagen strain nomenclature used in most databases, is the same as the protein named C16 protein in the Western Reserve strain of VACV that is the most studied member of this family. VACV also encodes an enzyme, B2/poxin that cleaves the second messenger cGAMP that is produced by cGAS and binds and activates STING [20,21], and E5 that is reported to bind directly to cGAS and target it for degradation [22].

We previously defined the function of the chicken cGAS/STING signalling axis in the sensing of the avipoxvirus, fowlpox virus (FWPV) [12], confirming the conservation of this pathway in sensing mammalian and avian poxviruses. In this study we asked two specific questions. Firstly, given that bird genomes encode cGAS and DNA-PK, but not IFI16, we asked whether DNA-PK functions as an innate sensor of exogenous DNA and DNA viruses in birds as it does in mammals [10,23,24]. Secondly, we analysed whether this fundamental mechanism of intracellular viral sensing is targeted by poxviruses that infect birds. Our data illustrate the importance of DNA-PK in sensing FWPV and exogenous DNA in chicken cells and determine the breadth of conservation of the mechanism encoded by poxviruses to inhibit DNA-PK-dependent DNA sensing. Surprisingly, we find that this mechanism of interfering with viral DNA sensing is the exists across more speies than other known methods by which poxviruses block intracellular DNA PRRs, cementing DNA-PK as a key component of anti-poxvirus immunity across different orders of life.

Results

DNA-PK is required for sensing viral DNA in chickens

DNA-PK consists of three subunits, DNA-PK catalytic subunit (DNA-PKcs, PRKDC/XRCC7), Ku70 (XRCC6) and Ku80 (XRCC5) functioning together as a heterotrimeric protein complex. Broad evolutionary analyses have identified homologues of DNA-PKcs, Ku70, and Ku80 across the eukaryotes and limited functional analysis in diverse lineages supports a conserved role in non-homologous end joining (NHEJ) double-strand DNA break repair [25–27]. These genes are therefore important for the maintenance of genomic stability and, in jawed vertebrates, for V(D)J recombination [28]. By sensing viral DNA, DNA-PK has another established function in innate immunity in humans and mice [10,24,29], but the degree of conservation of this function across taxa

is unexplored. We therefore first examined the distribution of the DNA-PK complex within the chordates, which contain the natural hosts of the economically important, and human infective, chordopoxvirus family. We sampled a range of chordate genomes covering this lineage, with a focus on major chordopoxvirus targets (birds, reptiles, mammals). The DNA-PK complex was identified in the majority of genomes examined and, in every bird, reptile, and mammal that we searched (Figure 1A). If the innate immune function of the DNA-PK complex is also conserved, as shown for humans and mice, then targeting this activity may also be important for poxvirus lineages beyond vaccinia virus. With this in mind, we next examined the specific target of the vaccinia virus C10/C16 protein, the Ku80 subunit of the DNA-PK complex. Ku80 shows high sequence level conservation across the chordates, particularly in the DNA binding domain, likely reflecting its important function in DNA repair (Figure 1B). We also note that this conserved DNA binding domain is the target of C10/C16 binding.

The Ku proteins and DNA-PKcs carry out NHEJ functions in chicken cells [30] but they have not been studied in the context of avian innate immune responses. To functionally assess the contribution of DNA-PK to intracellular DNA sensing in chickens we used the HD11 chicken macrophage cell line that has an active STING-dependent signalling pathway [12] to generate clonal Ku70 and DNA-PKcs knockout lines using CRISPR/Cas9 and confirmed the generated indels by sequencing across the target loci (Supplementary Figure 1A, B). During attempts to produce Ku70 knockout lines we noted that, despite multiple sgRNA guides targeting different exons being used, very few clones could be recovered, and those that were recovered were found to have background levels of cytokine and chemokine transcription that rendered the assessment of Ku70's role in DNA sensing intractable in this system (Figure 2A, B). We found DNA-PKcs to be transcribed in both chicken bone marrow derived macrophages and HD11 cells, and found its transcription to be upregulated by interferon alpha (IFN α) treatment (Supplementary Figure 2). We were able to generate multiple confirmed DNA-PKcs knockout lines that, in the resting state, did not have altered inflammatory gene transcription compared to parental lines. In these cells the DNA-dependent transcription of type-I interferon (*IFNB*) and *ISG12.2* was lost when compared to WT controls (Figure 2A, B). The transcription of *CCL4*, however, was unaffected by loss of DNA-PKcs (Figure 2C). In comparison, no defects were found in RNA-driven transcriptional responses in DNA-PKcs knockout cells (Figure 2D) consistent with a DNA-specific role for DNA-PK in intracellular nucleic acid sensing in chickens.

Wild-type poxviruses, including FWPV, often fail to induce an innate immune response due to the presence of a large number of intracellular PRR inhibitors [9,31]. Using a FWPV strain FP9 lacking an

immunomodulator (FPV012) that inhibits IFN-I production [13], we previously demonstrated that cGAS and STING are essential for sensing FWPV infection and that transcription of *ISG12.2* is a cGAS/STING-dependent signalling output in chicken cells [12]. Here we infected WT and DNA-PKcs^{-/-} macrophage cell lines with FWPVΔ012 strain and observed lower induction of *ISG12.2* transcription in DNA-PKcs^{-/-} cells compared with WT cells (Figure 2E). This data indicates that DNA-PKcs acts in concert with cGAS and STING in sensing FWPV infection in chicken cells in the same way that it does in mammals to sense VACV [10].

Chicken cells use a STING/TBK1/IRF7 pathway to sense DNA and FWPV infection

To further define the DNA-PK-dependent innate sensing pathway in chicken macrophages we used IRF7 knockout cells HD11 cells [32] and generated TBK1 HD11 knockouts. In mammals, following DNA stimulation, TBK1 phosphorylates STING and IRF3 allowing dimerisation nuclear translocation of IRF3 and subsequent IFN-I transcription. Chickens lack IRF3 but express an IRF7 with a C-terminus similar to mammalian IRF3 with a distribution of serine residues that mimic the mammalian TBK1 phosphorylation sites [32]. Knockout of TBK1 or IRF7 in HD11 cells resulted in a loss of DNA-driven *IFNB* and *ISG12.2* transcription (Figure 3A). Similarly the transcription *ISG12.2* in response to FWPVΔ12 infection was completely dependent on TBK1 and IRF7 (Figure 3B). These data, combined with our prior description of cGAS and STING knockout macrophages [12] indicate that chickens sense cytoplasmic DNA and FWPV infection via DNA-PK, and that this uses a canonical cGAS/STING/TBK1 pathway to drive IFN-I transcription with IRF7 as the dominant transcription factor. As such these core components of the intracellular DNA sensing pathway are highly conserved between mammals and birds.

The poxvirus C10/C4 family of Ku-binding proteins is highly conserved

Poxviruses use a plethora of immune modulators to inhibit PRR signalling and inhibit interferon production [14]. The C4 and C10/C16 proteins made by vaccinia virus bind directly to Ku and inhibit its ability to sense viral DNA [17–19]. Since the innate sensing function of DNA-PK is conserved across mammals and birds we postulated that the immune evasion mechanism used by the C4/C10 poxvirus family might also be conserved. We therefore used protein sequence homology searches to identify C4/C10 homologues and analyse their distribution across a broadly representative selection of poxviruses (Figure 4A). As previously reported, the B2/poxin family demonstrated the broadest distribution, being identified in mammalian and insect infective (entomopoxvirus) poxviruses [33].

However, the distribution of B2/poxin was extremely sparse beyond the orthopoxviruses and centapoxviruses. Of the other inhibitors examined, the C4/C10 family appeared the oldest, being present in the relatively early branching avipoxvirus family. Further examination of the relative positions of C4/C10 family genes within their respective genomes revealed that this family is almost exclusively localised to the genomic termini, either within or adjacent to the inverted terminal repeat (ITR) regions. These genomic regions are highly enriched in virulence genes, suggesting that a virulence mediating function may be conserved across the C4/C10 family (Supplementary Figure 3). This analysis of the conservation of C4/C10 family homologues indicates that this family is more highly conserved than the poxin (B2) and E5 families (Figure 4A) and suggest therefore that targeting DNA-PK may represent a broadly conserved and ancient strategy for poxvirus immune evasion, likely reflected in the conserved positioning of C4/C10 family genes within ITRs and genome termini.

We identified three C4/C10 family member genes in FWPV. This family contains a characteristic bi-domain structure (Figure 4B). The N-terminal domain is a structural mimic of the prolyl-hydroxylase family responsible for regulation of hypoxia-inducible factor 1 α (HIF-1 α) [34], while the C-terminal domain binds Ku70/80, blocking DNA binding to DNA-PK [18]. The C-terminal domain amino-acid sequence contains a distinctive 'LCYC' motif that is very highly conserved across family members and is structurally essential for the domain fold [17,19]. Two of these genes, 020 and 225, encode identical proteins and, like VACV C10/C16, are duplicate genes found in the inverted terminal repeats (ITR) of vaccinia that contain multiple duplicated genes. The third gene in FWPV is 006 which has a divergent sequence from 0200/255 but is still a member of the same family. To assess further the relationship between the poxviral C4/C10 family members we carried out a phylogenetic analysis of family members (Figure 4C). This analysis indicates that there have been multiple independent gene duplication events during the evolution of poxviruses that have led to many poxviruses carrying more than one copy of these genes. The duplication events, for example, that led to the appearance of C4 and C10/C16 in VACV occurred independently of the event that led to 020 and 006 in FWPV. This can be further evidenced by the presence of a C-terminal extension in all three FWPV proteins (006, 020, 225) that is not present in any of the orthopoxvirus family members (Supplementary Figure 4). As such there is a clear evolutionary pressure on most poxvirus families to maintain at least one copy, and in many cases multiple copies, of the C4/C10 family of immunomodulators.

Whilst it is true that the C4/C10 family is well conserved in terms of presence, examination of sequence level conservation across family members demonstrated a notable lack of strict sequence level conservation. The previously identified, highly conserved LCYC motif was indeed well conserved

across all of our identified genes, however the region of C10/C16 responsible for interacting with Ku80 and thus conferring inhibitory activity appeared only modestly conserved (Figure 4B). This prompted us to investigate experimentally the activity of the divergent avipoxvirus C4/C10 family proteins against their natural host DNA-PK.

The Fowlpox C4/C10 homologues 020 and 006 are immunomodulatory genes

To assess the conservation of function in the fowlpox C4/C10 homologues, we used the FWPVΔ020 and FWPVΔ006 deletion viruses and analysed previously generated microarray data from primary chicken embryonic fibroblasts (CEF) infected with these viruses [13]. We compared gene expression profiles of mutant strains to the wild-type fowlpox virus (FP9 strain), known for its disruption of DNA signalling pathways and suppression of interferon signalling in host cells [12,31,35]. Gene Ontology (GO) biological function analysis revealed significant differences in both knockout viruses compared to the FP9 strain, particularly in cell-to-cell signalling pathways (Figure 5A-B). We then screened the gene lists generated from the comparison between the knockout viruses and the wild-type virus for interferon and DNA-sensing immune response-related and cellular signalling transcripts [12,36]. This screening revealed that several genes, including *IFITM1*, *LY6E*, *MB21D1*, *IL6*, *FIB*, *TLR2-1*, *IFI30*, and *TNFAIP2*, were subtly but significantly upregulated in one or both of the knockout mutants compared to the wild-type FP9 FWPV strain (Figure 5C).

The identification of interferon-stimulated genes *IFITM1* and *Ly6E* as 020- and 006-regulated genes in FWPV-infected CEFs is consistent with the function of these genes as immunomodulatory proteins and regulators of FWPV-driven interferon production. To identify the upstream signals responsible for transcription of *IFITM1* and *Ly6E* we analysed DNA-stimulated WT and DNA-PKcs^{+/}, TBK1^{+/} and IRF7^{-/-} HD11 chicken macrophage cell lines. The DNA-driven induction of *IFITM1* and *Ly6E* transcription was dependent on DNA-PKcs, TBK1 and IRF7 (Figure 5D, E). Similarly infection of these cells with FWPVΔ012 indicated that transcription of both *IFITM1* and *Ly6E* are dependent on DNA-PKcs (Figure 5 F). Further, infection of chicken macrophages with FWPVΔ020 in WT cells showed that *IFITM1* and *Ly6E* transcription is upregulated in chicken cells during infection with FWPVΔ020, as in CEFs (Figure 5G). As such, the C4/C16 homologues in FWPV, 002 and 060 regulate the expression of genes that are dependent on the DNA-PK-driven intracellular signalling pathway and, as such, have the same function in FWPV as they do in VACV in inhibiting poxvirus DNA-driven innate immunity.

Blocking the DNA-Binding domain of Ku is a conserved mechanism of poxviral antagonism

The structure of VACV Western Reserve C16 (Copenhagen nomenclature: C10) bound to human Ku has been recently solved by CryoEM [17]. In this structure, a C16 (C10) homodimer was shown to engage the Ku70/80 heterodimer DNA binding region, specifically at the electropositive surface created by the dimer interface between Ku70 and Ku80 (Figure 6A, B- PDB:8AG5). Several loops in the C-terminal domain of C16 (C10) dimer come together to form a structure that binds the inner surface of the Ku DNA-binding ring (Figure 6B). Primary sequence analysis of the C4/C10 family, including the FWPV proteins 020 and 006, indicates that the amino-acids forming the Ku-binding loop are not conserved across species, suggesting the possibility of a different Ku-binding modality across different poxviruses. To assess this further, we first used AlphaFold2 (AF) to predict three-dimensional structures of the 020 and 006 proteins (Supplementary Figure 5). Both the N-terminal and C-terminal domains were predicted with high accuracy, but lower confidence was predicted in the loop between these domains and at the far C-terminus. The predicted structures of 020 and 006 suggest a highly conserved structure between these proteins and C10/C4. Dimeric assemblies of 020 and 006 were created by docking onto the VACV C16 structure, which overlays with very high confidence, indicating the potential for a conserved overall fold of these proteins. Furthermore, the loop regions of FWPV020 and 006 that are predicted to interact with chicken Ku70/80 have a distinctive electronegative surface that mimics the charge distribution on the equivalent region of C16 (C10) (Figure 6D). The conservation of this charge-distribution provides an explanation for the conservation of function of this family of proteins in the absence of strict primary sequence similarity conservation in the functional loop regions. To determine binding of these Fowlpox proteins to chicken Ku70/80, we used AF-Multimer to also predict the structure of Ku70/80. The structure was predicted with high confidence with the exception of the N and C-terminal regions which have flexible sections (Figure 6C and Supplementary Figure 5). To illustrate the electrostatic potential of the DNA binding pocket of Ku70/80, we truncated the N and C-terminal regions which are not involved in binding. From the electrostatic potential a strong electropositive patch can be visualised within the DNA-binding region (Figure 6C). This electropositive patch is utilised primarily for DNA binding, however the C4/C10 protein family have exploited this by creating proteins with high electronegativity to bind here and prevent DNA binding. This structural modelling offers a potential mechanistic basis for the functional observations from the FWPV 020 and 006 knockout viruses. Taken together, this strongly supports functional conservation of the C4/C10 protein family in Fowlpox and, by extension, across the avipox and orthopoxviruses.

Discussion

There are multiple DNA-sensing PRRs whose function contributes antiviral immunity. In general, these processes are poorly described in Sauropsida, including birds, compared to mammals, despite the ecological and economic importance of birds and their role as reservoirs of zoonotic viruses. To address this knowledge gap, we have recently described the role of cGAS/STING pathway in FWPV sensing [12] and the mechanisms of bacterial DNA sensing by TLR21 [32] in chickens. Here we extend our exploration of comparative immunology and host/poxvirus interactions by determining the contribution of DNA-PK to innate sensing of exogenous DNA and FWPV in chickens and highlight the conservation of the mechanism by which poxviruses inhibit this host response beyond the Mammalia taxon.

We found that the DNA-PK complex function in antiviral immunity is conserved between mammals and birds. Chicken cells lacking the catalytic subunit of DNA-PK, DNA-PKcs (encoded by the *PRKDC* gene) fail to produce IFN-I in response to DNA, but not RNA, and in response to poxvirus infection, equivalent to its function in mammals [10,24]. We also show that this response requires the kinase TBK1 and the transcription factor, IRF7. This data is consistent with IRF7 being a functional replacement for IRF3 in birds and the main IRF functioning downstream of PRRs in avian antiviral immunity [32,37]. As such, we have now demonstrated that the DNA-PK/cGAS/STING/IRF signalling pathway is highly conserved between birds and mammals. On the other hand, other mechanisms of viral DNA sensing, for example those that use the IF16 and AIM2 inflammasome protein family [38,39] are not used by birds as these loci are not present in avian species [40], which places to date the DNA-PK/cGAS/STING/IRF axis as the main DNA-sensing complex to be functionally available in birds.

All poxviruses produce multiple proteins that inhibit PRR-driven IFN-I production [14,15]. This is also true of avipoxviruses, since two FWPV proteins, FWPV012 and FWPV184, are known to reduce the amount of IFN-I and ISG transcription in infected chicken cells [13,31]. These two proteins are not thought to target DNA sensing PRRs directly, but rather to antagonise downstream signalling molecules. Here we add FPV020, FPV006 and FPV225 to the list of FWPV interferon antagonists and identify them as functional members of the poxvirus virus C4/C10 family. The conservation of this

family of poxviral immunomodulators is broader than that of B2 and E5, which target cGAMP and cGAS respectively (Figure 4A) [21,22]. This family is not only highly conserved, but, for unknown reasons, often has 2-3 copies per genome. VACV, for example, has two copies of C16/C10 (in its ITRs) and one copy of C4. Similarly FPV020 and FPV225 are identical genes and FPV006 is part of the same family. The presence of multiple copies of these genes, along with their high degree of conservation among poxviruses, may reflect their importance in the poxvirus life cycle. The C4/C10 protein family is multifunctional. VACV C16/C10 can activate the cellular hypoxic response via an interaction between its N-terminal domain and the host PHD2 protein that activates HIF-1a [34], and C4 can inhibit NF- κ B signalling via an unknown mechanism [41]. It remains to be understood whether the FWPV020 and 006 encode these functions as well as their function in blocking IFN-I production in chicken cells as described here. It is noteworthy that all identified C4/C10 family proteins share the two-domain structure with an N-terminal domain that mimics mammalian prolyl-hydroxylases [34] and a C-terminal domain that has a unique fold and is responsible for interactions with Ku [17,18]. This two-domain structure may be conserved in order to allow the dimerisation to occur that is necessary for Ku-binding, or there may be interdependent functions of the two domains that are not yet understood.

Poxviruses habitually acquire host genes by horizontal gene transfer mechanisms either directly recombination or DNA transposons, or indirectly by retrotransposons or retroviral transfer [42–45]. The copy number of these genes can be rapidly expanded, depending on the selective pressure experienced by the virus, and then the new genes evolved to provide later generations of virus with newly functional proteins [1,43]. This method often results in protein families in poxviruses with conserved domain structures (eg BCL-2-like, Ankyrin repeat, PRANC-domain proteins) [46–48]. Here the C-terminal domains of FWPV020 and 006 have the same fold (the same fold as VACV C4 and C10 C-terminal domains) in part due to the conserved LCYC motif [17,19]. The loops and surface-exposed residues, however, are very different, despite the Ku-binding loops maintaining the electronegative charges required for Ku-binding. This contrasts with the very high degree of conservation of the electropositive region of Ku targeted by this protein family. Targeting this conserved region of Ku is an immune evasion strategy that accommodates extensive plasticity in the C4/C10 protein family sequence, potentially allowing a large sequence space to be explored whilst retaining binding and at the same time limiting the options for host to mutate away. The success of this strategy is reflected in the conservation of the C4/C10 protein family across the poxviridae. The consistent presence of this family may also reflect a clear impact on virulence. In mouse models of VACV infection, C4 and C16/C10 knockout viruses are attenuated [41,49] and consistent with this is the presence of a

C4/C10 homologue in the more virulent clade 1b MPXV that is not present in the less virulent clade 2 virus [50].

It is estimated that the last common ancestor between avipoxviruses and orthopoxviruses split more than 200,000 years ago [51]. Combined with the consistent presence of DNA-PK inhibitors in vertebrate poxviruses, our analyses here imply that inhibition of DNA-PK is an ancient immune evasion mechanism employed by this family of viruses. Given the presence of viral proteins found to targeting DNA-PK in multiple dsDNA viruses [52] it is likely that this mechanism of innate immune evasion is also conserved across different virus families. Similar to the recent understanding of the ancient nature of cGAS signalling [53], it is clear that evolutionarily ancient mechanisms of host nucleic acid sensing are present across taxa along with viral inhibitory mechanisms that have resulted in increasingly complex mechanisms of innate sensing in mammals. As such, understanding the differences in PRRs and their variation across taxa could guide future research in wildlife immunology and significantly enhance our ability to predict the zoonotic potential of various animal hosts.

Material and Methods

Reagents

Calf Thymus (CT) DNA (Sigma) and Herring Testes (HT) DNA (Sigma), polyinosinic-polycytidyllic acid (poly(I:C), Invivogen), were diluted in nuclease-free water (Ambion, ThermoFisher).

Cell Culture

HD11 cells, an avian myelocytomatosis virus (MC29)-transformed chicken macrophage-like cell line, were incubated at 37°C, 5% CO₂. They were grown in RPMI (Sigma-Aldrich, Germany) complemented with 2.5% volume per volume (v/v) heat-inactivated foetal bovine serum (FBS; Sera Laboratories International Ltd), 2.5% volume per volume (v/v) chicken serum (New Zealand origin, Gibco, Thermo Fisher Scientific), 10% Tryptose Phosphate Broth solution (Gibco, Thermo Fisher Scientific), 2 mM L-glutamine (Gibco, Thermo Fisher Scientific), 50 µg/ml of penicillin/streptomycin (P/S; Gibco, Thermo Fisher Scientific). Chicken embryonic fibroblasts (CEFs) (Pirbright Institute, Woking) were incubated at 37°C, 5% CO₂ and were grown in Dulbecco's Modified Eagle Medium (DMEM) -F12 with Glutamax (Gibco), 5% v/v FBS, and 50 µg/ml P/S. Chicken bone marrow derived macrophages (BMDM) were generated as previously described (17). Briefly, femurs and tibias of 4 week-old immunologically mature White Leghorn (PA12 line) outbred chickens were removed, both

ends of the bones were cut and the bone marrow was flushed with RPMI supplemented with P/S. Cells were then washed and re-suspended in RPMI, loaded onto an equal volume of Histopaque-1077 (Sigma-Aldrich, Germany), and centrifuged at 400 g for 20 min. Cells at the interface were collected and washed twice in RPMI. Purified cells, pooled from three homozygous chickens, were seeded in triplicates at 1×10^6 cells/ml in sterile 60 mm bacteriological petri dishes in RPMI supplemented with 10% FBS, 25 mM HEPES, 2 mM L-glutamine, P/S and 25 ng/ml recombinant chicken colony stimulating factor 1 (CSF-1) (Kingfisher Biotech, Inc) at 41°C and 5% CO₂. Half of the medium was replaced with fresh medium containing CSF-1 at day 3. At day 6, adherent cells were harvested and cultured in RPMI supplemented with 10% FBS, 25 mM HEPES, 2 mM L-glutamine, and P/S prior to stimulation.

HD11 knockout generation by CRISPR-Cas9

CRISPR guide RNAs were designed according to the *Gallus gallus* *PKRDC* (DNA-PKcs) and *XRCC6* (Ku70) sequences obtained from the Ensembl database (release 94), single guide (sg)RNA sequences were designed targeting exon boundaries. Genome editing of HD11 was performed using ribonucleoprotein (RNP) delivery. tracrRNA was mixed with the target specific sgRNA (Table 1), followed by an incubation at 95°C. To form the RNP complex, the tracrRNA/sgRNA mix was incubated with the Cas9 protein (IDT, Leuven, Belgium) and electroporation enhancer at 21°C. To generate knockout cells, 1×10^6 cells per guide were electroporated with the corresponding RNP complex using Lonza Electroporation Kit V (Lonza). After 48 h, the cells were expanded for future experiments and their DNA were extracted using the PureLink Genomic DNA Kit (Thermo Scientific, Waltham, MA, USA). The knockout efficiency was evaluated by genotyping the polyclonal cell populations using MiSeq (Illumina) according to a published method. The successfully edited populations were diluted to a concentration of 0.5 cell/well and seeded in 96-well plates. Individual clones were sequenced by MiSeq and the confirmed knockout clones were expanded for experiments (Supplementary Figure 1).

Stimulation Assays

HD11 cells were seeded in 12-well plates at a density of 3×10^5 cells/well. In the following day, the cells were transfected using Transit-LT1 (Mirus Bio, USA) with CT-DNA (1, 2, or 5 µg/ml) or Poly(I:C) (1 µg/ml), and harvested 6 or 16 h post-transfection. In the priming assays, IFN α (200 ng/ml) was added 16 h prior to transfection.

RNA Extraction

Cells were lysed by overlaying with 250 µl of lysis buffer containing 4 M guanidine thiocyanate, 25 mM Tris pH 7, and 143 mM 2-mercaptoethanol. As a second step, 250 µl of ethanol was added, and the solution was transferred to a silica column (Epoch Life Science, Inc., Sugar Land, TX, USA) and centrifuged; all centrifugation steps were performed for 90 s at 16,600 g. The bound RNA was washed by centrifugation with 500 µl of buffer containing 1 M guanidine thiocyanate, 25 mM Tris pH 7, and 10% ethanol, followed by a double washing step with 500 µl of wash buffer 2 [25 mM Tris pH 7 and 70% (v/v) ethanol]. RNA was eluted by centrifugation in 30 µl of nuclease-free water and the concentration was measured using a NanoDrop 2000 Spectrophotometer (Thermo Scientific, Waltham, MA, USA).

cDNA and qPCR

Using 500 ng of RNA extracted from HD11 cells, cDNA was produced using SuperScript III reverse transcriptase, following the manufacturer's protocol (Thermo Scientific, Waltham, MA, USA). Samples were diluted in nuclease-free water in a 1:2.5 ratio. One µl of the diluted product was used for quantitative PCR (qPCR) in a final volume of 10 µl. qPCR was performed using SybrGreen Hi-Rox (PCR Biosystems Inc.) using primers described in Table 1. Fold change in mRNA expression was calculated by relative quantification using hypoxanthine phosphoribosyltransferase (HPRT) as endogenous control.

Table 1 qRT-PCR primer sequences.

Gene name	Forward sequence	Reverse sequence
GAPDH	GTCCTCTCTGGCAAAGTCCAAG	CCACAACTACTCAGCACCTGC
HPRT	TGGTGGGGATGACCTCTCAA	GGCGATATCCCACACTTCG
IFNB	TCCTGCAACCATCTTCGTCA	CACGTCTTGTGGCAAG
ISG12-2	TGACCAGAACGTCCACAAAGCCG	ACCTGCTCCTGGACCGATGCTT
CCL4	CCTGCTGCACCACTTACATAACA	GCGCTCCTCTTGTGATGAA
IFITM1	GTGAAGTCCAGGGATCGCAA	GATCAGATGGGCCGTGATGT
Ly6E	CATCTCAAAGGCTGCTCTCC	GCCGCAATGCCGAGGTTAAT
MAP2K4	GACGAGGCGTTATGGTTCT	TTGCCCACTTGGTTGTGGA
PRKDC	CTTGAGGGTGTGGTCAA	TAAGGCCAGCTTAAACGCA

Fowlpox Virus Growth and Titration

FWPV WT (FP9) and mutants were propagated in primary chicken embryonic fibroblasts (CEFs) and grown in DMEM-F12 (Thermo Fisher Scientific, Waltham, MA, USA) containing 1% FBS and 5% P/S, and harvested 5 days later. Ten-fold dilutions of cell supernatants were prepared in serum-free DMEM-F12 and used to inoculate confluent monolayers of CEFs for 1.5 h at 37°C. Cells were then overlaid with 2xMEM: CMC (1/1 ratio). The plaques were counted seven days later after fixation. For infection experiments HD11 cells were seeded in 12-well plates in the day prior to infection. Fowlpox viruses were diluted in serum-free DMEM-F12 at a multiplicity of infection (MOI) of 3 and added in the cells (1 ml per well). Infected cells and supernatants were collected from infections at 16h and 24h post-infection.

Homology searching and databases

Identification of PRR pathway inhibitors in poxviridae. A broadly representative panel of 54 complete reference poxvirus genomes was selected from the Bacterial and Viral Bioinformatic Resource Center (<https://www.bv-brc.org>). Vaccinia sequences for the protein families of interest were searched against predicted proteomes derived from this genome panel using BLASTp at low stringency (e-value cut off 0.1, max hits 500). Putative homologues were confirmed by reciprocal best BLASTp into the vaccinia proteome, followed by sequence alignment and, where relevant, examination of predicted domain structure. A further, iterative, HMM-based search strategy was employed to ensure that no detectable homologues had been missed. Using the vaccinia sequences as the seed, iterative HMMER (<http://hmmer.org>) searches were carried out against the entire uniprotKB database. These searches were run until convergence or divergence and results filtered to identify poxviridae derived sequences. These searches returned no additional homologues from the genome panel initially selected suggesting that our initial search had captured all identifiable homologues.

Identification of DNA-PK subunits in chordates.

A representative panel of chordate genomes with a focus on groups widely associated with poxvirus infection (reptiles, birds, mammals) was selected (Supplementary Table 1). Human DNA-PKcs, Ku70, and Ku80 were searched against predicted proteomes from these genomes using BLASTp with default settings. Putative homologues were validated via reciprocal BLASTp into the human proteome. Where no homologous proteins were identified within a taxa a phylogenetically close

taxa was also searched in order to reduce the possibility of false negatives. In all cases where we failed to identify protein homologues within a genome the same was true of sister taxa.

Phylogenetic reconstruction of C4/C10 family

Phylogenetic analysis was carried out as previously described [32]. Briefly, Sequences were aligned in Jalview with MAFFT (L-INS-I)[54,55]. Informative sites identification and alignment trimming was carried out with TrimAl (Strict settings) [56]. Subsequent substitution model selection (ModelFinder[57]) and phylogenetic reconstruction was carried out in IQ-Tree [56].

Microarray/RNAseq

The original microarray data used in this study have been previously published [13] and deposited in accordance with MIAME guidelines in the public database ArrayExpress (<http://www.ebi.ac.uk/microarray-as/ae/>; Acc. No: E-MTAB-7276). Data were reanalyzed at both the probe and gene levels using the Transcriptome Analysis Console (TAC) 4.0 software from Affymetrix. Microarray data were analysed with default settings, where a gene was considered expressed in a particular condition if it was detected in 50% or more of the samples with a Detection Above Background (DABG) *p*-value of less than 0.05. Additionally, a threshold of a 1.5-fold change in expression was applied to identify differentially expressed genes.

Pathway analysis

Differentially regulated genes underwent Gene Ontology (GO) analysis, which classified associated mechanisms into biological processes (BP) and dot plot visualisation was done using ShinyGO (v0.80; [58]). A False Discovery Rate (FDR) *p*-value threshold of <0.05 was used as a standard metric to quantify the most closely related GO terms. The heatmap illustrating gene expression patterns was generated using the seaborn library (v0.13) for advanced visualisation in Python 3.8+, with additional customization provided by matplotlib (v3.9.0).

Protein structure prediction

AlphaFold2 (AF) was used for predicting the structures of FWPV006 and FWPV020 and AF2-Multimer for Gallus Gallus Ku70/80 heterodimer [59]. The top ranked hit for each was assessed for its confidence score and coloured according to AF prediction confidence. The dimeric assemblies of FWPV006 and FWPV020 were created by docking the N- and C-terminal domains onto the structure of C16 (C10) due to their similarity and the inability of AF to correctly predict these accurately. All structural figures including electrostatics were made using ChimeraX [60].

Statistical analysis

Prism 9 (GraphPad) was used to generate graphs and perform statistical analysis. Data were analysed using an unpaired t test with Welch's correction unless stated otherwise. Data with $P < 0.05$ was considered significant and 2-tailed P-value were calculated and presented as: * $p < 0.05$, ** $p < 0.01$, *** $p < 0.001$; **** $p < 0.0001$. Each experiment has at least two biological replicates unless stated.

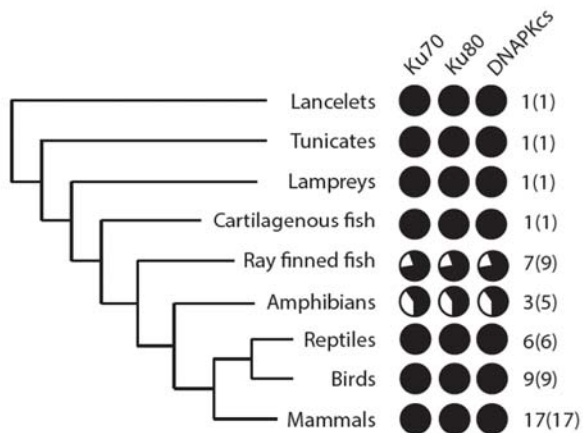
Acknowledgements

This work was funded by BBSRC grants BB/S001336/1 (BF and CB), BB/E009956/1, BB/G018545/1, BB/H005323/1 & BB/K002465/1 (MS) and by EUROFERI (Région Centre-Val-de-Loire, France, RG).

Figures

Figure 1

A



B

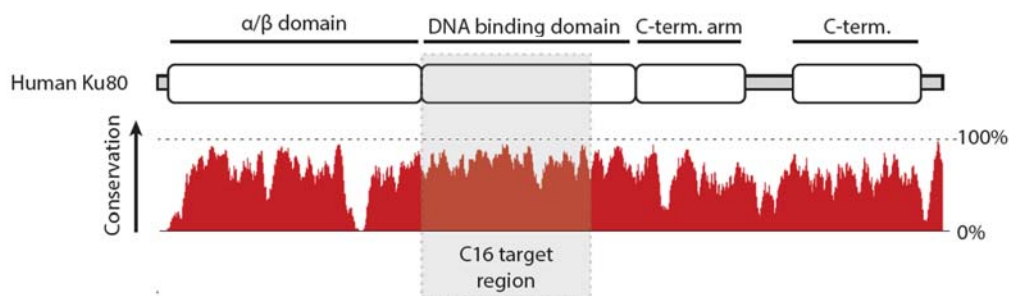


Figure 1. Conservation of the DNA-PK complex. A) Degree of conservation of Ku70, Ku80 and DNA-PKcs genes across chordates. Numbers indicate the presence of genes found in each taxonomic group compared with the number of species searched. B) Amino-acid level conservation of Ku80 across chordates. Domain structure of Ku80 is shown above and amino-acid percentage conservation shown below. The region of Ku80 targeted by VACV C16 (C10) protein is shown in grey.

Figure 2

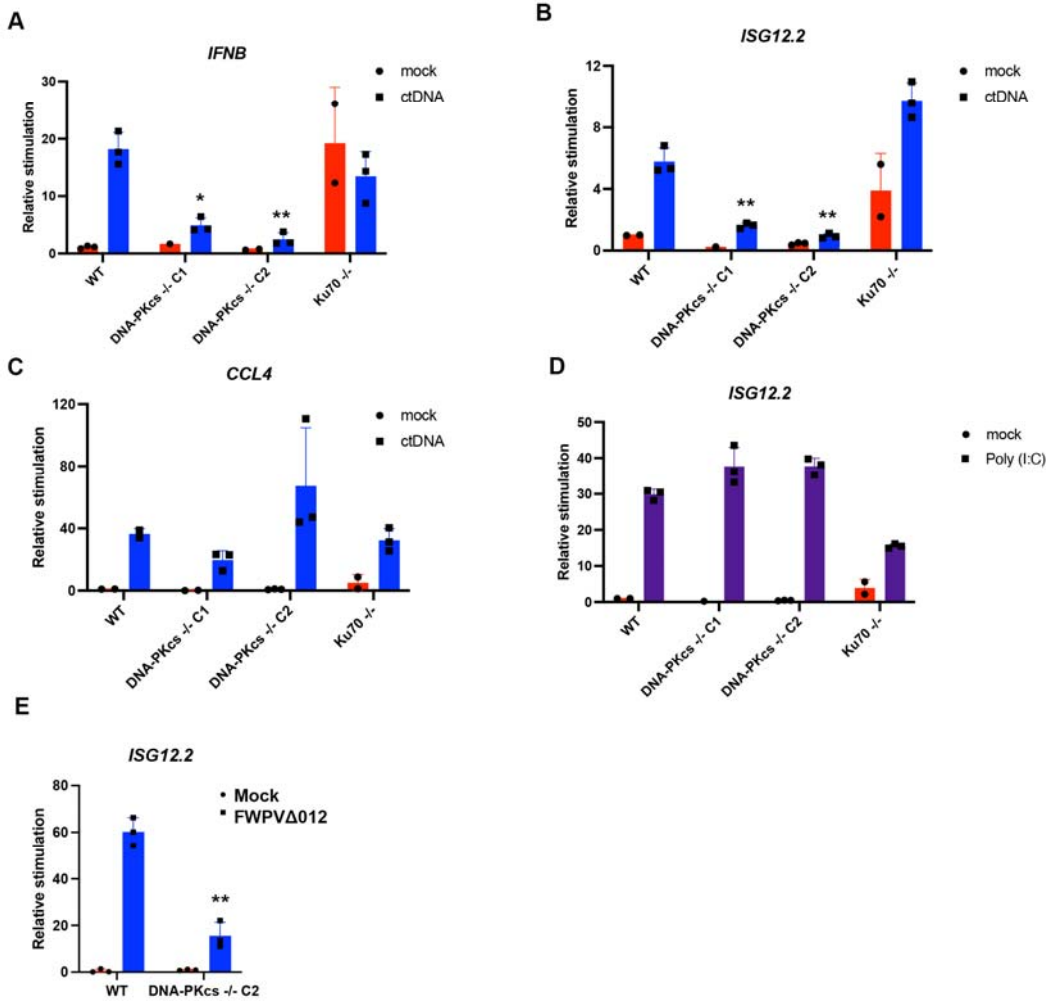


Figure 2. DNA and Fowlpox sensing is impaired in DNA-PKcs knockout chicken cells. WT, DNA-PKcs^{-/-} or Ku70^{-/-} HD11 cells were stimulated with CT-DNA (5 µg/ml) and transcription of A) *IFNB*, B) *ISG12.2* and C) *CCL4* were measured by qRT-PCR 6 h later. D) WT, DNA-PKcs^{-/-} or Ku70^{-/-} HD11 cells were stimulated with Poly(I:C) (2 µg/ml) and transcription of *ISG12.2* was measured by qRT-PCR 6 h later. E) WT or DNA-PKcs^{-/-} cells were infected with FWPVΔ012 and *ISG12.2* was measured by qRT-PCR 24 h later. Data is presented as mean ± SEM and analysed by two-tailed Student's T test with n = 3; *p < 0.05, **p < 0.01.

Figure 3

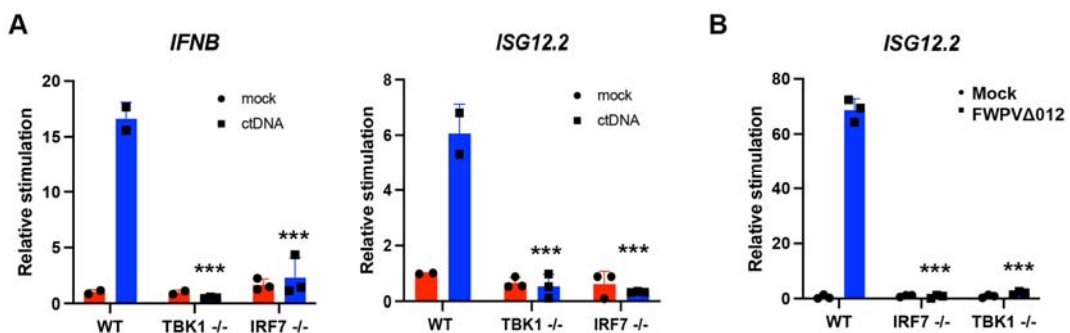
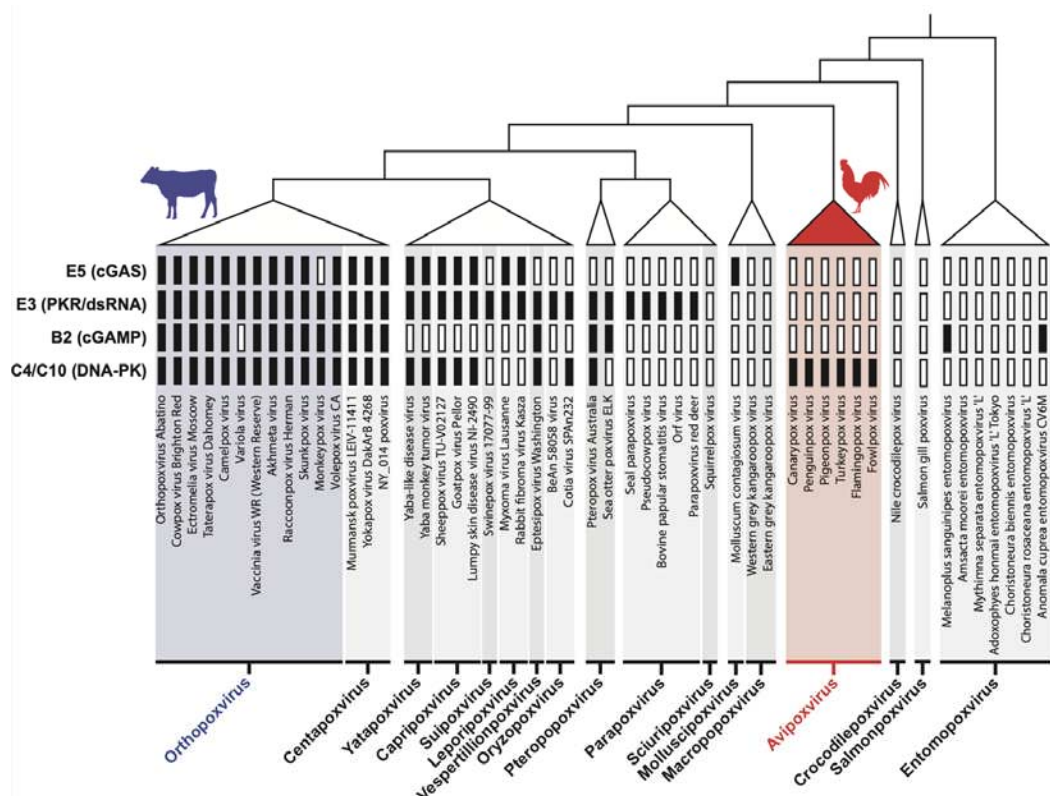


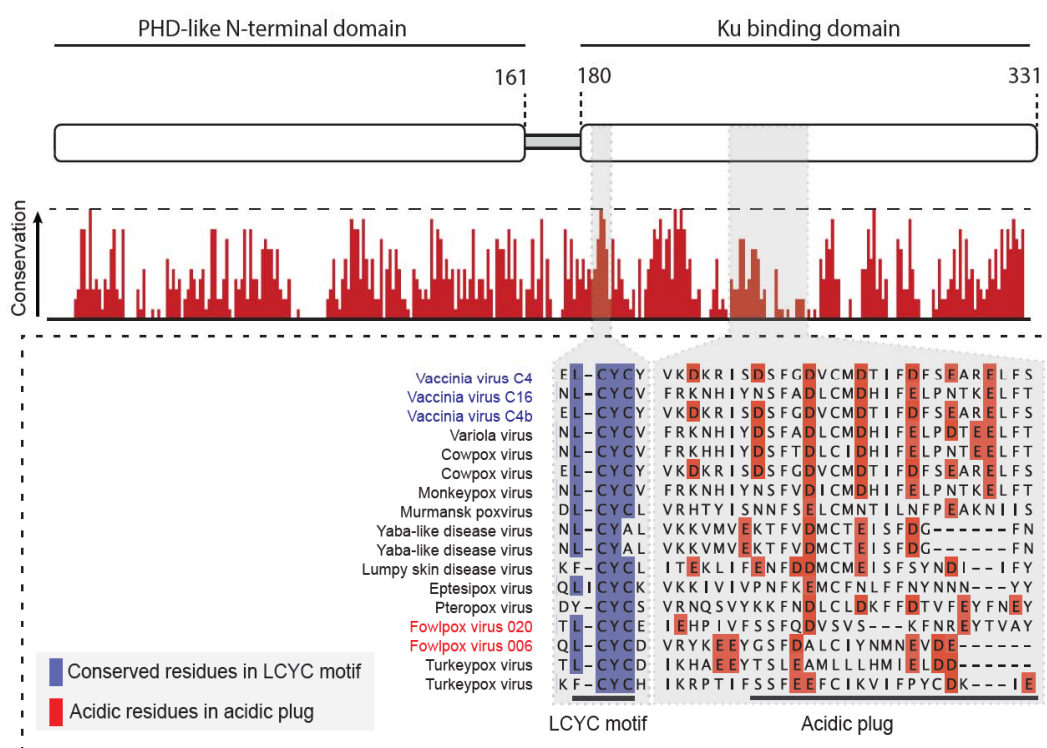
Figure 3: Fowlpox sensing by DNA-PKcs / TBK1 / IRF7. A) WT, TBK1^{-/-} or IRF7^{-/-} HD11 cells were stimulated with CT-DNA (5 µg/ml) and transcription of *IFNB* and *ISG12.2* were measured by qRT-PCR 6 h later. B) WT, TBK1^{-/-} or IRF7^{-/-} HD11 cells were mock infected or infected with FWPVΔ012 and *ISG12.2* was measured by qRT-PCR 24 h later. Data is presented as mean ± SEM and analysed by two-tailed Student's T test with n = 3; ***p < 0.01.

Figure 4

A



B



C

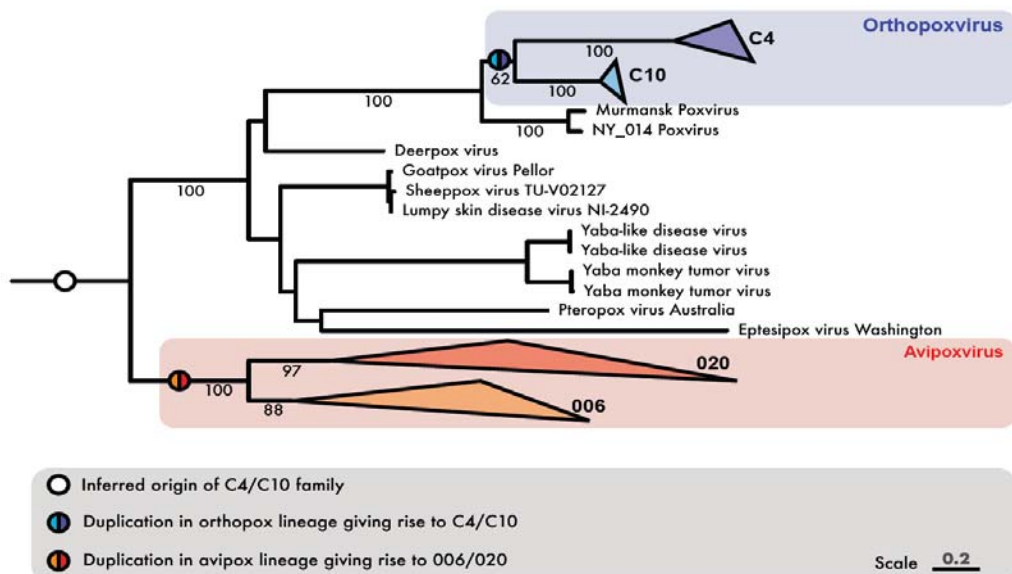


Figure 4. The C4/C10 family of poxvirus immunomodulators is highly conserved across species A)
 Gene-level conservation of poxviral immunomodulators B2, C4/C10, E3 and E5 across poxviridae. B) Amino-acid level conservation across the C4/C10 protein. Domain structure of C4/C10 (top) with % amino acid conservation below, specifically highlighting the highly conserved LCYC motif and the variability across the acidic plug that binds Ku. C) Phylogenetic tree of C4/C10 family, branch labels represent ultrafast bootstrap support at key nodes.

Figure 5

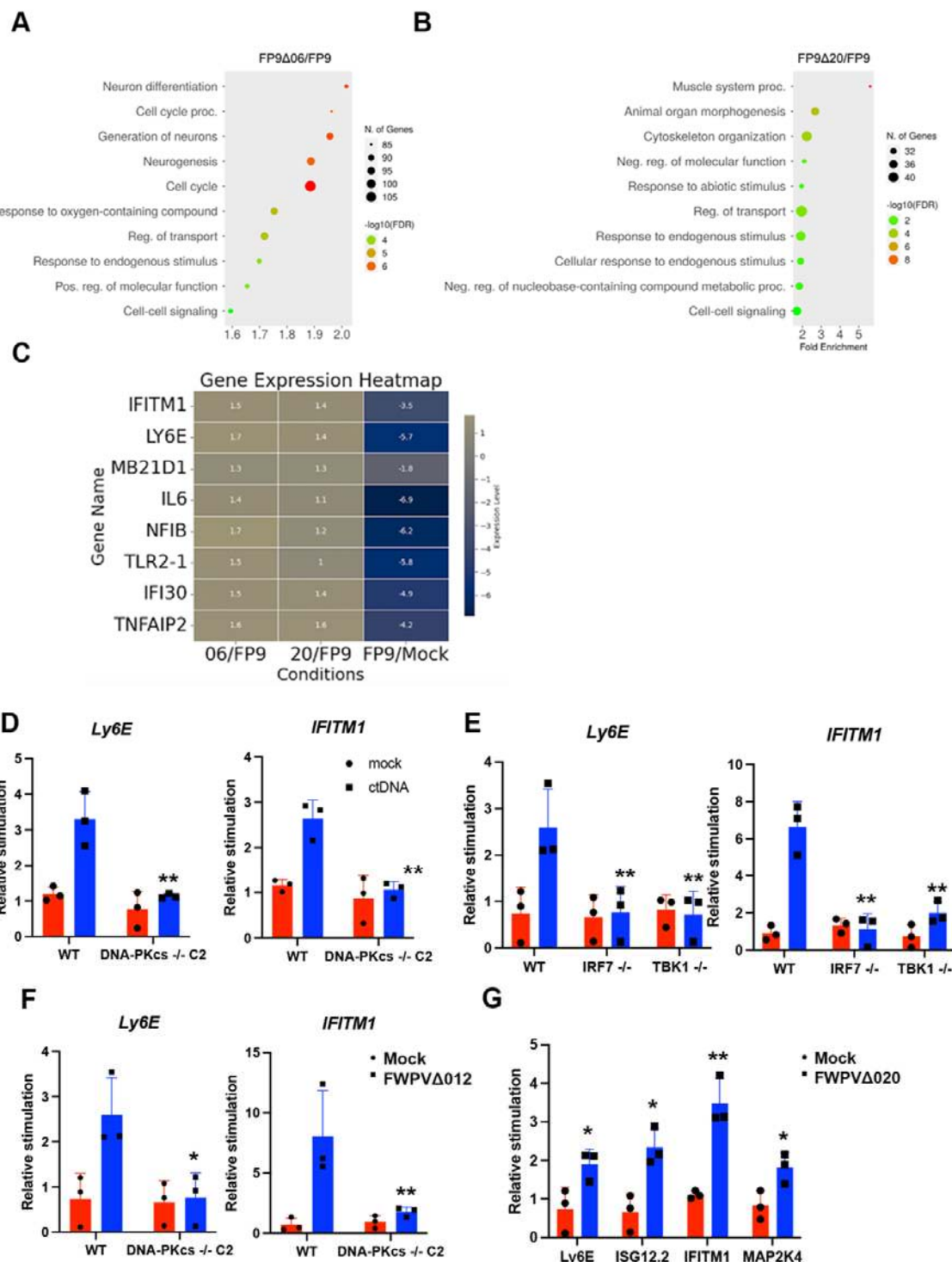


Figure 5. FWPV genes 006 and 020 negatively regulate the IFN-I response during FWPV infection

A and B) Gene Ontology (GO) analysis using ShinyGO identified the top 10 enriched pathways in comparisons between FP9Δ06 vs. FP9 and FP9Δ020 vs. FP9, depicted as dot plots (Figures A and B, respectively). Dot size reflects the number of genes, and colour indicates the significance level (-log10(FDR)). C) A heatmap illustrating selected immune gene expression levels across conditions FWPVΔ006 vs. FP9, FWPVΔ020 vs. FP9, and FP9/Mock, generated using Python's pandas, seaborn (v0.13), and matplotlib (v3.9.0). Axes display comparisons and gene names, while a colour bar provides a scale for gene expression levels. D) WT or DNA-PKcs^{-/-} HD11 cells were stimulated with CT-DNA (5 µg/ml) and transcription of *Ly6E* and *IFITM1* were measured by qRT-PCR 6 h later. E) WT or DNA-PKcs^{-/-} cells were mock infected or infected with FWPVΔ012 and *Ly6E* and *IFITM1* were measured by qRT-PCR 24 h later. F) WT, TBK1^{-/-} or IRF7^{-/-} HD11 cells were stimulated with CT-DNA (5 µg/ml) and transcription of *Ly6E* and *IFITM1* were measured by qRT-PCR 6 h later. G) HD11 cells were mock infected or infected with FWPVΔ020 and *Ly6E*, *ISG12.2*, *IFITM1* and *MAP2K4* were measured by qRT-PCR 24 h later. Data is presented as mean ± SEM and analysed by two-tailed Student's T test with n = 3; \square p < 0.05, $\square\blacksquare$ p < 0.01.

Figure 6

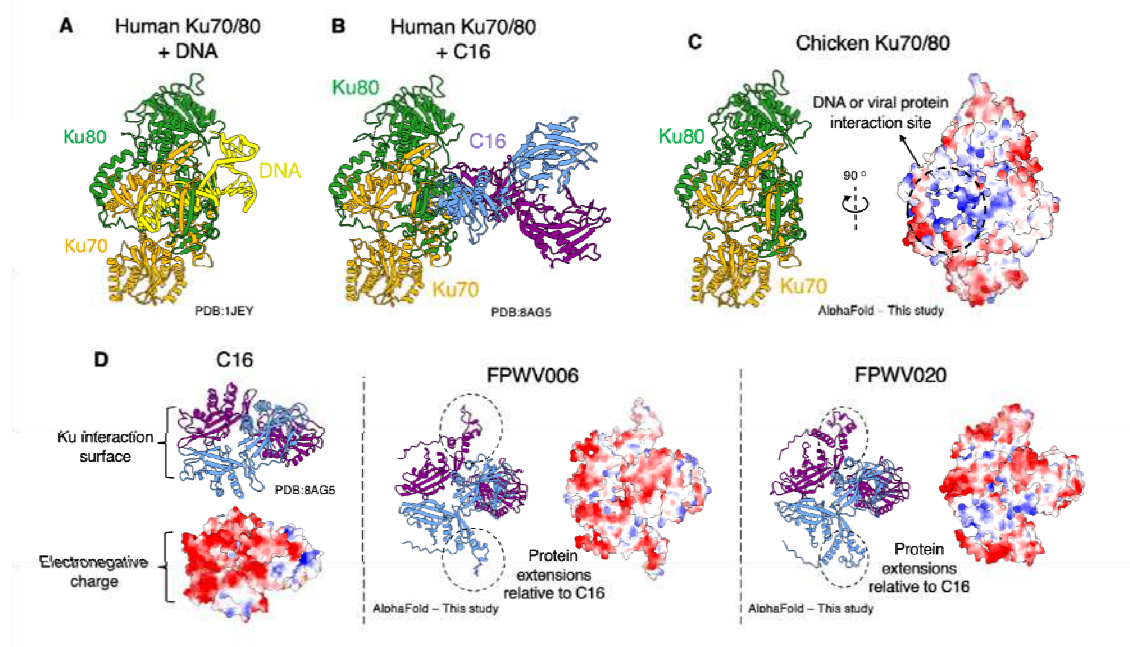


Figure 6: Structural analysis and comparison of FWPV006 and FWPV020 with VACV C16 (C10). A) X-ray crystallography structure of human Ku70/80 with DNA (PDB:1JEY) (Walker, 2001), Ku70 in orange, Ku80 in green and DNA in yellow. B) Human Ku70/80 with VACV WR C16 (C10) (PDB:8AG5) (Rivera-Calzada et al., 2022), Ku70 in orange, Ku80 in green, C16 (C10) in blue and purple. C) AlphaFold prediction of Chicken Ku70/80 (orange/green) and an electrostatic surface representation of the DNA or viral protein electropositive patch. D) Structures of C16 (C10) (PDB:8AG5), AlphaFold models of FWPV006 and FWPV020 in purple and blue with electrostatic surface comparisons.

Supplementary Figures and Legends

XRCC6 KO indels

Reference GCCA**TGTTCGAGCCCTACGAGGATGAGGAG**
67% reads GCCATGT-CGAGCCCTACGAGGATGAGGAG
18% reads GCCATGT--GAGCCCTACGAGGATGAGGAG

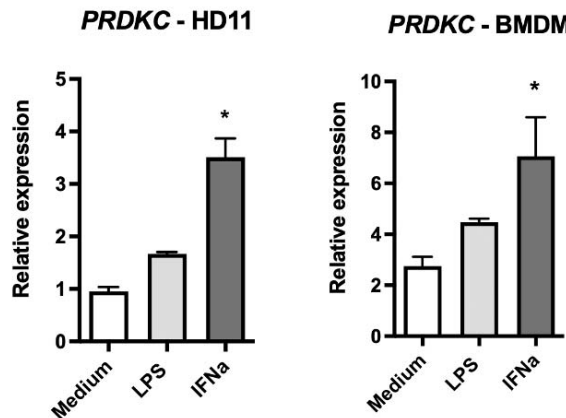
PRKDC KO C1 indels

Reference TTCTGTTCTGCCAGGAGGG**CCTTGTTG** GAAGATGAGCACAT**TCT** CCTGAAGCTT
67% reads TTCTGTTCTGCCAGGAGGGC-----ACATCTCCTGAAGCTT
18% reads TTCTGTTCTGCCAGGAGGGC**TTTG** | T | GAAGATGAGCACATCTCCTGAAGCTT

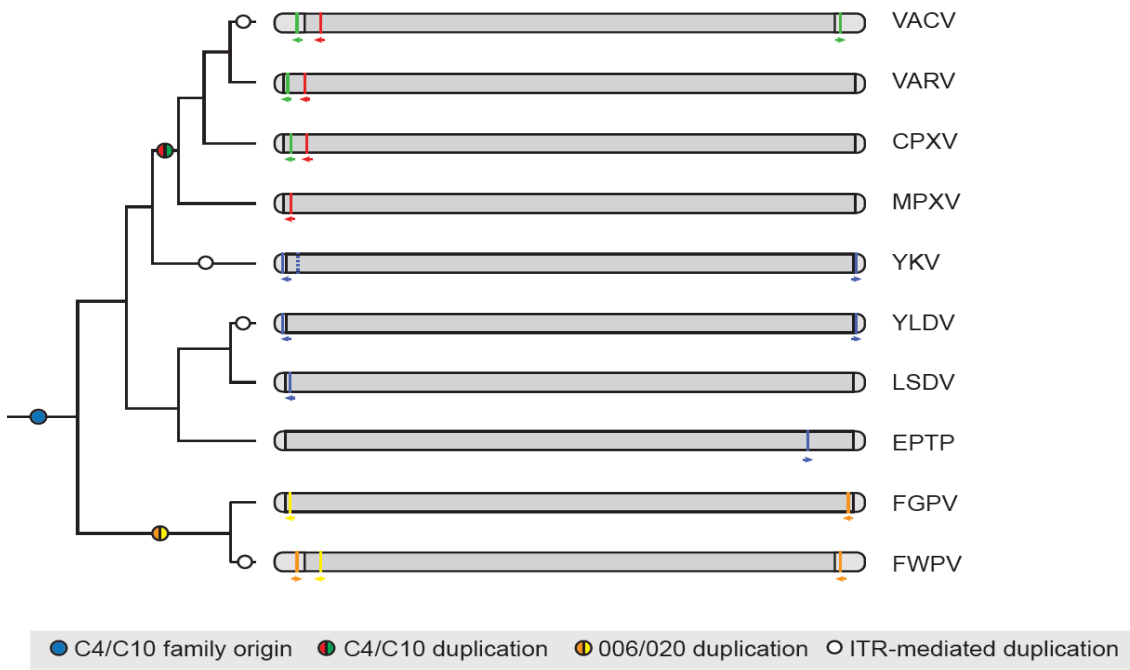
PRKDC KO C2 indels

Reference TTCTGTTCTGCCAGGAGGG**CCTTG** GAAGATGAGCACAT**TCT** CCTGAAGCTT
50% reads T-----GAAGATGAGCACATCTCCTGAAGCTT
22% reads TTCTGTTCTGCCAGGAGGG**CTTG** -----GATGAGCACATCTCCTGAAGCTT

Supplementary Figure 1: Ku70 and DNA-PKcs knockout HD11 cell lines were generated by CRISPR/Cas9 editing and sequenced to define indels targeted by the gRNAs (yellow) including PAM sequences (red).



Supplementary Figure 2: DNA-PKcs expression is enhanced by interferon treatment in chicken cells. HD11 or BMDM cells were treated with 10 nM LPS or 50 μ M IFN α for 6 hours and the level of PRKDC mRNA was measured by RT-qPCR. $p < 0.01$, $n=3$. Data is presented as mean \pm SEM and analysed by two-tailed Student's T test with $n = 3$; * $p < 0.05$.



Supplementary Figure 3: Genomic locations of C4/C10 family genes in selected poxviruses.

Coloured bands represent individual gene positions, arrows denote direction of open reading frame.

C16	$\xrightarrow{\beta 1}$	TT	$\xrightarrow{\beta 2}$	20	999	al	999	30						
C16	1	10	20	999	999	30							
C4	.MDIYDDKG	LQT	IKLEN	.NEFD	DCI	RNDI	REL	FKHVT	..					
FPv006	.MEFSCTGTNNQ	LAV	BRE	.TETR	TSF	.ELVNLG	.ISD	LNDIK	NICE	.SKIF	FPEKR	TE			
FPv020	.MSEFTYIRD	DG	I	PK	MHIES	.DYF	.SDE	NKL	.LIKIE	ETN	.MDY	DFESES	RIL	DEHT	GE

Sequence alignment showing the positions of beta-sheets β_3 , β_4 , β_5 , and β_6 across four proteins: C16, C4, FPv006, and FPv020. The alignment highlights the beta-sheets with blue boxes and their positions with arrows above the sequence.

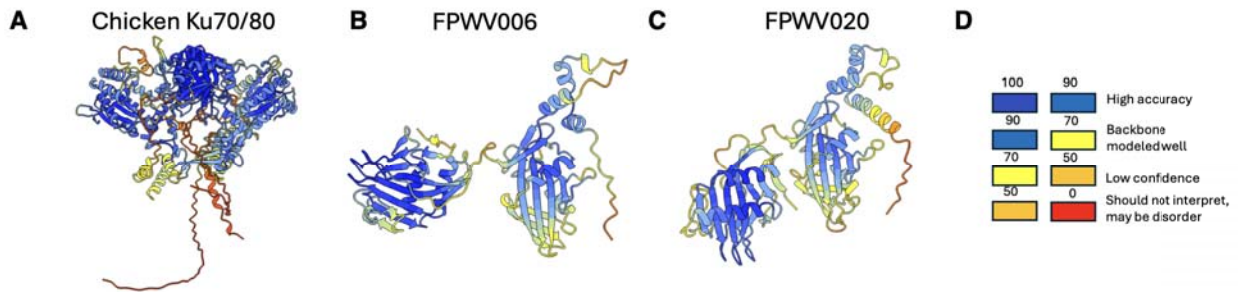
The diagram illustrates the proteolytic processing of the C16 protein. C16 is a single polypeptide chain. It is cleaved by β 16 at position TT (residues 219-220) to yield fragment C16. C16 is then cleaved by β 17 at position TT (residues 229-230) to yield fragments C16 and C4. C16 is further cleaved by β 18 at position TT (residues 240-241) to yield fragments C16, C4, and FPv006. Finally, C16 is cleaved by β 19 at position TT (residues 250-251) to yield fragments C16, C4, FPv020, and FPv006. The fragments are color-coded: C16 (blue), C4 (green), FPv006 (red), and FPv020 (purple).

Sequence alignment of C16, C4, FPv006, and FPv020. The alignment shows the C16 protein structure with a beta2I domain (red) and a C-terminal domain (blue). The beta2I domain is highlighted in red, and the C-terminal domain is highlighted in blue. A red arrow above the sequence indicates the beta2I domain, and a blue arrow below the sequence indicates the C-terminal domain. A black arrow above the sequence indicates the C16 protein structure. A red asterisk at the bottom indicates a stop codon.

C16
C16
C4
FPV006 **F**NIVRGNALLEEDNEY.**GCD**
FPV020 **F**KIVLSKOEVYDLOSDESDSDITDND

Supplementary Figure 4: Structure based sequence alignment of VACV and FWPV C4/C10 homologues

Secondary structure-guided amino-acid sequence alignments were generated based on PDB:8AG5 and AlphaFold models. Conserved residues are shown in red. Green boxes are Ku-binding loops. Blue stars indicate residues predicted to be involved in dimerisation.



Supplementary Figure 5: AlphaFold predictions of chicken Ku70/80 and FWPV006 and FWPV020.

A) AlphaFold-Multimer prediction of chicken Ku70/80 coloured according to D. B) AlphaFold prediction of FWPV006 coloured according to D. C) AlphaFold prediction of FWPV020 coloured according to D. D) Key of AlphaFold prediction confidence.

References

1. Elde NC, Child SJ, Eickbush MT, Kitzman JO, Rogers KS, Shendure J, et al. Poxviruses Deploy Genomic Accordions to Adapt Rapidly against Host Antiviral Defenses. *Cell*. 2012;150: 831–841.
2. Koonin, E and Dolja V. A virocentric perspective on the evolution of life. *Curr Opin Virol*. 2013;3: 546–557.
3. Duggal NK, Emerman M. Evolutionary conflicts between viruses and restriction factors shape immunity. *Nat Rev Immunol*. 2012;12: 687–695.
4. Enard D, Cai L, Gwennap C, Petrov DA. Viruses are a dominant driver of protein adaptation in mammals. 2016 [cited 27 Jul 2024]. doi:10.7554/eLife.12469
5. Mansur DS, Smith GL, Ferguson BJ. Intracellular sensing of viral DNA by the innate immune system. *Microbes Infect*. 2014;16: 1002–1012.
6. Bryant CE, Orr S, Ferguson B, Symmons MF, Boyle JP, Monie TP. International Union of Basic and Clinical Pharmacology. XCVI. Pattern recognition receptors in health and disease. *Pharmacol Rev*. 2015;67: 462–504.
7. Li X-D, Wu J, Gao D, Wang H, Sun L, Chen ZJ. Pivotal roles of cGAS-cGAMP signaling in antiviral defense and immune adjuvant effects. *Science*. 2013;341: 1390–1394.
8. Lam E, Stein S, Falck-Pedersen E. Adenovirus detection by the cGAS/STING/TBK1 DNA sensing cascade. *J Virol*. 2014;88: 974–981.
9. Georgana I, Sumner RP, Towers GJ, Maluquer de Motes C. Virulent Poxviruses Inhibit DNA Sensing by Preventing STING Activation. *J Virol*. 2018;92. doi:10.1128/JVI.02145-17
10. DNA-PKcs is required for cGAS/STING-dependent viral DNA sensing in human cells. *iScience*. 2024;27: 108760.
11. Dai P, Wang W, Cao H, Avogadri F, Dai L, Drexler I, et al. Modified vaccinia virus Ankara triggers type I IFN production in murine conventional dendritic cells via a cGAS/STING-mediated cytosolic DNA-sensing pathway. *PLoS Pathog*. 2014;10: e1003989.
12. Oliveira M, Rodrigues DR, Guillory V, Kut E, Giotis ES, Skinner MA, et al. Chicken cGAS Senses Fowlpox Virus Infection and Regulates Macrophage Effector Functions. *Front Immunol*. 2020;11: 613079.
13. Giotis ES, Laidlaw SM, Bidgood SR, Albrecht D, Burden JJ, Robey RC, et al. Modulation of Early Host Innate Immune Response by an Avipox Vaccine Virus' Lateral Body Protein. *Biomedicines*. 2020;8. doi:10.3390/biomedicines8120634
14. Smith GL, Benfield CTO, de Motes CM, Mazzon M, Ember SWJ, Ferguson BJ, et al. Vaccinia virus immune evasion: mechanisms, virulence and immunogenicity. *Journal of General Virology*. 2013. pp. 2367–2392. doi:10.1099/vir.0.055921-0
15. Seet BT, Johnston JB, Brunetti CR, Barrett JW, Everett H, Cameron C, et al. Poxviruses and immune evasion. *Annu Rev Immunol*. 2003;21: 377–423.

16. El-Jesr M, Teir M, de Motes CM. Vaccinia Virus Activation and Antagonism of Cytosolic DNA Sensing. *Frontiers in Immunology*. 2020; :.
17. Rivera-Calzada A, Arribas-Bosacoma R, Ruiz-Ramos A, Escudero-Bravo P, Boskovic J, Fernandez-Leiro R, et al. Structural basis for the inactivation of cytosolic DNA sensing by the vaccinia virus. *Nat Commun*. 2022;13: 7062.
18. Peters NE, Ferguson BJ, Mazzon M, Fahy AS, Krysztofinska E, Arribas-Bosacoma R, et al. A mechanism for the inhibition of DNA-PK-mediated DNA sensing by a virus. *PLoS Pathog*. 2013;9: e1003649.
19. Scutts SR, Ember SW, Ren H, Ye C, Lovejoy CA, Mazzon M, et al. DNA-PK Is Targeted by Multiple Vaccinia Virus Proteins to Inhibit DNA Sensing. *Cell Rep*. 2018;25: 1953–1965.e4.
20. Hernández B, Alonso G, Georgana I, El-Jesr M, Martín R, Shair KHY, et al. Viral cGAMP nuclease reveals the essential role of DNA sensing in protection against acute lethal virus infection. *Sci Adv*. 2020;6:.
21. Eaglesham JB, Pan Y, Kupper TS, Kranzusch PJ. Viral and metazoan poxins are cGAMP-specific nucleases that restrict cGAS-STING signalling. *Nature*. 2019;566: 259–263.
22. Yang N, Wang Y, Dai P, Li T, Zierhut C, Tan A, et al. Vaccinia E5 is a major inhibitor of the DNA sensor cGAS. *Nat Commun*. 2023;14: 2898.
23. Ku proteins promote DNA binding and condensation of cyclic GMP-AMP synthase. *Cell Rep*. 2022;40: 111310.
24. Ferguson BJ, Mansur DS, Peters NE, Ren H, Smith GL. DNA-PK is a DNA sensor for IRF-3-dependent innate immunity. 2012 doi:10.7554/eLife.00047
25. Uncovering DNA-PKcs ancient phylogeny, unique sequence motifs and insights for human disease. *Prog Biophys Mol Biol*. 2021;163: 87–108.
26. Tamura K, Adachi Y, Chiba K, Oguchi K, Takahashi H. Identification of Ku70 and Ku80 homologues in *Arabidopsis thaliana*: evidence for a role in the repair of DNA double-strand breaks. *Plant J*. 2002;29: 771–781.
27. Nenarokova A, Záhonová K, Krasilnikova M, Gahura O, McCulloch R, Zíková A, et al. Causes and Effects of Loss of Classical Nonhomologous End Joining Pathway in Parasitic Eukaryotes. *MBio*. 2019;10. doi:10.1128/mBio.01541-19
28. Kulesza P. DNA-dependent Protein Kinase in V(D)J Recombination: Reconstitution of the Scid Defect by Human DNA-PK CDNA. 1999.
29. Sui H, Zhou M, Imamichi H, Jiao X, Sherman BT, Lane HC, et al. STING is an essential mediator of the Ku70-mediated production of IFN-λ1 in response to exogenous DNA. *Sci Signal*. 2017;10. doi:10.1126/scisignal.aaah5054
30. Abe T, Ishiai M, Hosono Y, Yoshimura A, Tada S, Adachi N, et al. KU70/80, DNA-PKcs, and Artemis are essential for the rapid induction of apoptosis after massive DSB formation. *Cell Signal*. 2008;20: 1978–1985.
31. Laidlaw SM, Robey R, Davies M, Giotis ES, Ross C, Buttigieg K, et al. Genetic screen of a mutant poxvirus library identifies an ankyrin repeat protein involved in blocking induction of avian type

I interferon. *J Virol.* 2013;87: 5041–5052.

32. Guabiraba R, Rodrigues DR, Manna PT, Chollet M, Saint-Martin V, Trapp S, et al. Mechanisms of type I interferon production by chicken TLR21. *Dev Comp Immunol.* 2024;151: 105093.
33. Eaglesham JB, McCarty KL, Kranzusch PJ. Structures of diverse poxin cGAMP nucleases reveal a widespread role for cGAS-STING evasion in host-pathogen conflict. *Elife.* 2020;9. doi:10.7554/eLife.59753
34. Mazzon M, Peters NE, Loenarz C, Krysztofinska EM, Ember SWJ, Ferguson BJ, et al. A mechanism for induction of a hypoxic response by vaccinia virus. *Proc Natl Acad Sci U S A.* 2013;110: 12444–12449.
35. Giotis ES, Skinner MA. Spotlight on avian pathology: fowlpox virus. *Avian Pathol.* 2019;48: 87–90.
36. Giotis ES, Robey RC, Skinner NG, Tomlinson CD, Goodbourn S, Skinner MA. Chicken interferome: avian interferon-stimulated genes identified by microarray and RNA-seq of primary chick embryo fibroblasts treated with a chicken type I interferon (IFN- α). *Vet Res.* 2016;47: 75.
37. Cheng Y, Zhu W, Ding C, Niu Q, Wang H, Yan Y, et al. IRF7 Is Involved in Both STING and MAVS Mediating IFN- β Signaling in IRF3-Lacking Chickens. *J Immunol.* 2019;203: 1930–1942.
38. Unterholzner L, Keating SE, Baran M, Horan KA, Jensen SB, Sharma S, et al. IFI16 is an innate immune sensor for intracellular DNA. *Nat Immunol.* 2010;11: 997–1004.
39. Hornung V, Ablasser A, Charrel-Dennis M, Bauernfeind F, Horvath G, Caffrey DR, et al. AIM2 recognizes cytosolic dsDNA and forms a caspase-1-activating inflammasome with ASC. *Nature.* 2009;458: 514–518.
40. Cridland JA, Curley EZ, Wykes MN, Schroder K, Sweet MJ, Roberts TL, et al. The mammalian PYHIN gene family: phylogeny, evolution and expression. *BMC Evol Biol.* 2012;12: 140.
41. Ember SWJ, Ren H, Ferguson BJ, Smith GL. Vaccinia virus protein C4 inhibits NF- κ B activation and promotes virus virulence. *J Gen Virol.* 2012;93: 2098–2108.
42. Bratke KA, McLysaght A. Identification of multiple independent horizontal gene transfers into poxviruses using a comparative genomics approach. *BMC Evol Biol.* 2008;8: 67.
43. Brennan G, Stoian AMM, Yu H, Rahman MJ, Banerjee S, Stroup JN, et al. Molecular Mechanisms of Poxvirus Evolution. *MBio.* 2023;14: e0152622.
44. Hughes, A and Friedman, R. Poxvirus genome evolution by gene gain and loss. *Mol Phylogenet Evol.* 2005;35: 186–195.
45. Fixsen SM, Cone KR, Goldstein SA, Sasani TA, Quinlan AR, Rothenburg S, et al. Poxviruses capture host genes by LINE-1 retrotransposition. *Elife.* 2022;11. doi:10.7554/eLife.63332
46. Boys IN, Johnson AG, Quinlan MR, Kranzusch PJ, Elde NC. Structural homology screens reveal host-derived poxvirus protein families impacting inflammasome activity. *Cell Rep.* 2023;42: 112878.
47. Mutz P, Resch W, Faure G, Senkevich TG, Koonin EV, Moss B. Exaptation of Inactivated Host Enzymes for Structural Roles in Orthopoxviruses and Novel Folds of Virus Proteins Revealed by

Protein Structure Modeling. MBio. 2023;14: e0040823.

48. Graham SC, Bahar MW, Cooray S, Chen RA-J, Whalen DM, Abrescia NGA, et al. Vaccinia virus proteins A52 and B14 Share a Bcl-2-like fold but have evolved to inhibit NF-kappaB rather than apoptosis. *PLoS Pathog.* 2008;4: e1000128.
49. Fahy AS, Clark RH, Glyde EF, Smith GL. Vaccinia virus protein C16 acts intracellularly to modulate the host response and promote virulence. *J Gen Virol.* 2008;89: 2377–2387.
50. Forni D, Cagliani R, Molteni C, Clerici M, Sironi M. Monkeypox virus: The changing facets of a zoonotic pathogen. *Infect Genet Evol.* 2022;105: 105372.
51. Babkin IV, Babkina IN. Molecular dating in the evolution of vertebrate poxviruses. *Intervirology.* 2011;54: 253–260.
52. Hristova DB, Lauer KB, Ferguson BJ. Viral interactions with non-homologous end-joining: a game of hide-and-seek. *J Gen Virol.* 2020;101: 1133–1144.
53. Li Y, Slavik KM, Toyoda HC, Morehouse BR, de Oliveira Mann CC, Elek A, Levy S, Wang Z, Mears KS, Liu J, Kashin D, Guo X, Mass T, Sebé-Pedrós A, Schwede F, Kranzusch PJ. cGLRs are a diverse family of pattern recognition receptors in innate immunity. *Cell.* 2023;186: 3261–3276.e20.
54. Waterhouse AM, Procter JB, Martin DMA, Clamp M, Barton GJ. Jalview Version 2--a multiple sequence alignment editor and analysis workbench. *Bioinformatics.* 2009;25: 1189–1191.
55. Katoh K, Standley DM. MAFFT multiple sequence alignment software version 7: improvements in performance and usability. *Mol Biol Evol.* 2013;30: 772–780.
56. Capella-Gutiérrez S, Silla-Martínez JM, Gabaldón T. trimAl: a tool for automated alignment trimming in large-scale phylogenetic analyses. *Bioinformatics.* 2009;25: 1972–1973.
57. Kalyaanamoorthy S, Minh BQ, Wong TKF, von Haeseler A, Jermiin LS. ModelFinder: fast model selection for accurate phylogenetic estimates. *Nat Methods.* 2017;14: 587–589.
58. Ge SX, Jung D, Yao R. ShinyGO: a graphical gene-set enrichment tool for animals and plants. *Bioinformatics.* 2020;36: 2628–2629.
59. Jumper J, Evans R, Pritzel A, Green T, Figurnov M, Ronneberger O, et al. Highly accurate protein structure prediction with AlphaFold. *Nature.* 2021;596: 583–589.
60. Meng EC, Goddard TD, Pettersen EF, Couch GS, Pearson ZJ, Morris JH, et al. UCSF ChimeraX: Tools for structure building and analysis. *Protein Sci.* 2023;32: e4792.